Available online at www.sciencedirect.com

SciVerse ScienceDirect

Nuclear Physics A 910–911 (2013) 421–424

NUCLEAR PHYSICS A

www.elsevier.com/locate/nuclphysa

# Measurement of jet spectra in Pb-Pb collisions at $\sqrt{s_{NN}}$=2.76 TeV with the ALICE detector at the LHC

Marta Verweij (for the ALICE collaboration)[a]

[a] *Utrecht University*

**Abstract**

We report a measurement of transverse momentum spectra of jets detected with the ALICE detector in Pb-Pb collisions at $\sqrt{s_{\rm NN}}$=2.76 TeV. Jets are reconstructed from charged particles using the anti-$k_{\rm T}$ jet algorithm. The background from soft particle production is determined for each event and subtracted. The remaining influence of underlying event fluctuations is quantified by embedding different probes into heavy-ion data. The reconstructed transverse momentum spectrum is corrected for background fluctuations by unfolding. We compare the inclusive jet spectra reconstructed with $R = 0.2$ and $R = 0.3$ for different centrality classes and compare the jet yield in Pb–Pb and pp events.

*Keywords:* jet quenching, Hard Probes

## 1. Jet Reconstruction with charged particles in ALICE

For this analysis data collected by the ALICE experiment in the heavy-ion run of the LHC in the fall of 2010 with an energy $\sqrt{s_{\rm NN}} = 2.76$ TeV are used. Jets are clustered from charged particles reconstructed using the central tracking detectors Inner Tracking System (ITS) and Time Projection Chamber (TPC). This ensures a uniform acceptance in full azimuth and $|\eta| < 0.9$.

For signal jets the anti-$k_{\rm T}$ algorithm [1] is used and for background clusters the $k_{\rm T}$ algorithm [2]. For this analysis jet radii of $R = 0.2$ and 0.3 were used. The minimum $p_{\rm T}$ of the jet constituents is 0.15 GeV/$c$. All jets with a jet axis within $|\eta| < 0.5$ are considered for this analysis. The average background density per unit area $\rho$ is estimated event-by-event by calculating the median $p_{\rm T}/A$ (with $A$ the area of the jet) of all except the two leading $k_{\rm T}$ clusters in the event. From each signal anti-$k_{\rm T}$ jet in the event $\rho \cdot A$ is subtracted from the reconstructed $p_{\rm T}$ of the jet [3, 4].

## 2. Unfolding

ALICE has measured background fluctuations induced by the underlying event in heavy-ion collisions and studied the contributing sources [3]. Background fluctuations have a large impact on the measured jet spectrum due to the tail to upwards fluctuations in the $\delta p_{\rm T}$ distribution. The fluctuations are corrected for by unfolding. A response matrix $RM_{\delta p_{\rm T}}$ containing the $p_{\rm T}$ smearing due to background fluctuations is constructed from the measured $\delta p_{\rm T}$ distribution.

*Email address:* marta.verweij@cern.ch (Marta Verweij (for the ALICE collaboration))



0375-9474/ 
http://dx.doi.org/10.1016/j.nuclphysa.2012.12.105

Detector effects affecting the jet energy resolution are the charged particle tracking efficiency and the transverse momentum resolution. The efficiency is the dominant contributor to the jet energy resolution. The tracking efficiency has been studied with the detector simulation using Pythia and HIJING. The magnitude of the correction of detector effects is a 10% shift in the jet energy scale which corresponds to 40% on the jet yield assuming the jet spectrum scales with $p_T^{-5}$. The uncertainty on the exact knowledge of the tracking efficiency results in a 3% uncertainty on the jet energy scale reported in the systematic uncertainty of the measurement.

The two response matrices from background fluctuations and detector effects are combined to obtain the response matrix which will be used in the unfolding procedure: $M = RM_{\delta p_T} \cdot RM_{det} \cdot T$ in which $M$ is the measured jet yield and $T$ is the true jet yield.

Jet spectra are unfolded using a $\chi^2$ minimization method. Using this method the number of jets is always conserved. The $\chi^2$ function to be minimized indicates how well the unfolded distribution convoluted with the response matrix (the refolded spectrum) describes the measured spectrum. The $\chi^2$ function used in this analysis is:

$$\chi^2 = \sum_{\text{refolded}} \left( \frac{y_{\text{refolded}} - y_{\text{measured}}}{\sigma_{\text{measured}}} \right)^2 + \beta \sum_{\text{unfolded}} \left( \frac{d^2 log\ y_{\text{unfolded}}}{d\ log\ p_{\text{T}}^2} \right)^2, \quad (1)$$

in which $y$ is the yield of the refolded, measured or unfolded jet spectrum and $\sigma_{\text{measured}}$ the statistical uncertainty on the measured jet spectrum. The first summation term of equation 1 gives the $\chi^2$ between the refolded spectrum and the measured jet spectrum. The second summation term of equation 1 is the penalty term which is used to regularize the unfolded solution and favors a local power law. Regularization is necessary to avoid heavily fluctuating solutions. The strength of the applied regularization $\beta$ is tuned so as to make sure the regularization term is not dominant. In case the regularization is dominant the penalty term is equal to or larger than the $\chi^2$ between the refolded and measured spectrum. In this case the refolded spectrum does not describe the measured spectrum. In case the regularization is too weak or too strong off-diagonal correlations in the Pearson coefficients extracted from the covariance matrix are observed.

The regularization adds a systematic uncertainty of $\sim$ 10% for central events and $\sim$ 4% for peripheral events to the unfolded yield .

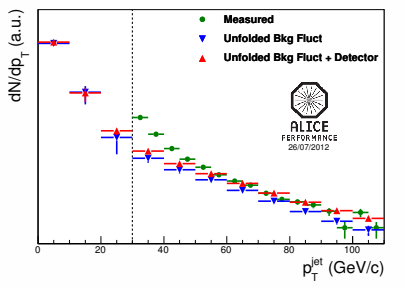


Figure 1: Unfolded spectra after correction for background fluctuations and the combined correction for background fluctuations and detector effects are shown. The dotted vertical line at $p_T = 30$ GeV/$c$ indicates the minimum $p_T$ cut-off of the measured spectrum.

**Transverse momentum range to optimize**

The measured spectrum is only used between a minimum and maximum transverse momentum, $p_{\text{T}}^{\text{min,meas}}$ and $p_{\text{T}}^{\text{max,meas}}$. The maximum $p_T$ cut-off is driven by the available statistics. The minimum $p_T$ cut-off is introduced to suppress clusters from the soft background which do not originate from a hard process. These soft clusters dominate the low $p_T$ part of the jet spectrum. The optimal value of the minimum $p_T$ cut-off has been studied in a model in which a jet spectrum as in vacuum is folded with the measured background fluctuations and using the jet background model described in [5, 6]. The minimum $p_T$ cut off on the measured spectrum is typically $5\sigma(\delta p_T)$ in which $\sigma(\delta p_T)$ is the width of the $\delta p_T$ distribution.

**Transverse momentum range of unfolded spectrum**

In the unfolding it is allowed to redistribute the yield of the measurement below the minimum $p_{\mathrm{T}}$ cut-off on the measured spectrum. Combinatorial clusters with $p_{\mathrm{T}} > p_{\mathrm{T}}^{\mathrm{min,meas}}$ in the measured spectrum will appear in the low $p_{\mathrm{T}}$ region of the unfolded spectrum. The low $p_{\mathrm{T}}$ region of the unfolded spectrum also allows feed-in from $p_{\mathrm{T}} < p_{\mathrm{T}}^{\mathrm{min,meas}}$ into the region where the $\chi^2$ is minimized. Feed-in from larger transverse momenta than the maximum measured momentum is also allowed by extending the reach of the unfolded spectrum to $p_{\mathrm{T}} = 250$ GeV/$c$.

The unfolding will break down if the fit gets too much freedom which is when the number of fitting parameters, number of bins in the unfolded spectrum, are similar or larger than the number of bins in the measurement.

Figure 1 illustrates the different $p_{\mathrm{T}}$ ranges for the measured and unfolded spectrum. In this example there are 16 bins in the measured spectrum and 11 in the unfolded. The unfolded spectrum below $p_{\mathrm{T}}^{min,meas}$ is not used in the measurement.

## 3. Results

The corrected differential jet spectrum normalized by the number of collisions $N_{\mathrm{coll}}$ reconstructed from charged particles in heavy-ion collisions with jet radius $R = 0.3$ and constituents $p_{\mathrm{T}} > 0.15$ GeV/$c$ is shown in Figure 2(a). A centrality evolution for the yield of jets is observed. Figure 2(b) shows the jet nuclear modification factor $R_{AA}^{Pythia}$ for which a jet spectrum from Pythia-Perugia[7] has been used as a reference. For the nuclear modification factor a simulated reference is used due to the limited statistics in the pp minimum bias data at $\sqrt{s_{\mathrm{NN}}}$=2.76 TeV. A strong jet suppression is observed for central events. For more peripheral events the suppression decreases. This implies that the full jet energy is not captured by jets with radii 0.2 and 0.3 in heavy-ion events. This is also observed in the jet $R_{CP}$ as shown in Figure 3(a) where the jet spectrum measured in 50-80% centrality has been used as a reference.

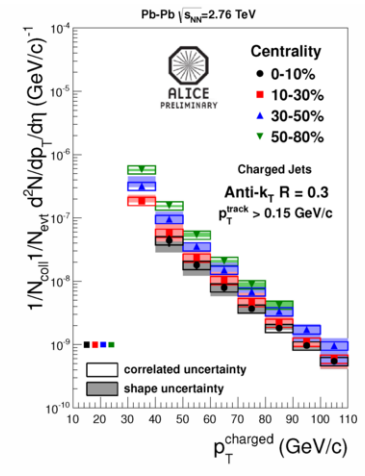


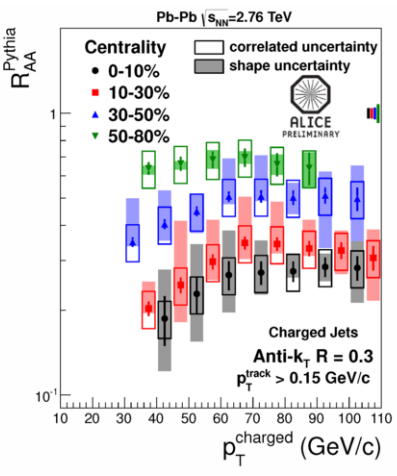


(b) $R_{AA}^{Pythia}$ for jet radius $R = 0.3$. For the reference jet spectrum Pythia Perugia0 is used.

Figure 2: Unfolded jet spectra and nuclear modification factor $R_{AA}^{Pythia}$ for jets reconstructed with radius $R = 0.3$.

Figure 3(b) shows that the ratio between the measured jet spectra for radii of $R = 0.2$ and $R = 0.3$ is consistent with jet production in vacuum for central and peripheral events. No significant jet broadening between radii of 0.2 and 0.3 is observed in the ratio of the cross sections.

The charged jet results of ALICE are compared to the JEWEL jet quenching MC [8, 9] in Figure 4. A good agreement is observed between the energy loss implementation of JEWEL and the charged jet results from ALICE.

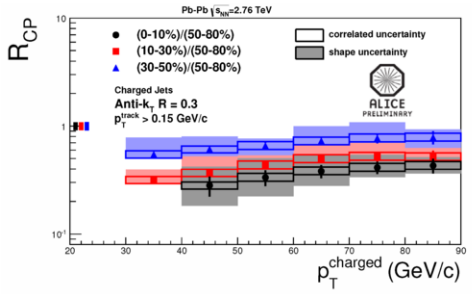


(a) $R_{CP}$ for jet radius $R = 0.3$. The peripheral jet spectrum corresponds to 50-80% centrality.

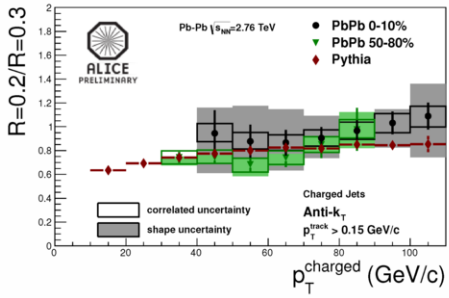


(b) Ratio between $R = 0.2$ and $R = 0.3$ Pb–Pb jet spectra compared to Pythia.

Figure 3: Jet $R_{CP}$ and ratio between $R = 0.2$ and $R = 0.3$ jet spectra.

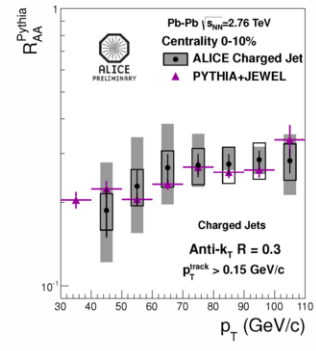


(a) Comparison between JEWEL and measured charged jet $R_{AA}$ for jet radius $R = 0.3$.

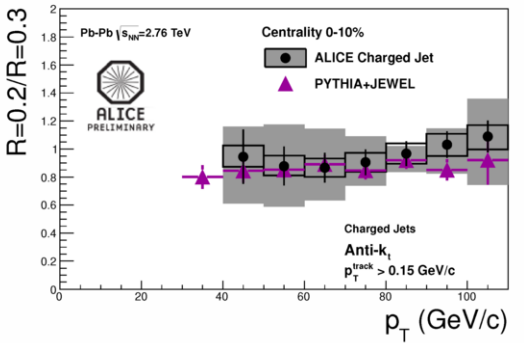


(b) Ratio between $R = 0.2$ and $R = 0.3$ Pb–Pb jet spectra compared to JEWEL.

Figure 4: Comparison of data and JEWEL energy loss MC.

## References


[1] M. Cacciari, G. P. Salam, G. Soyez, The anti-kt jet clustering algorithm, JHEP 0804 (2008) 063.
[2] M. Cacciari, G. P. Salam, Dispelling the $n^3$ myth for the kt jet-finder, Phys.Lett.B 641 (2006) 57–61. arXiv:hep-ph/0512210.
[3] B. Abelev, et al., Measurement of Event Background Fluctuations for Charged Particle Jet Reconstruction in Pb-Pb collisions at $\sqrt{s_{NN}} = 2.76$ TeV, JHEP 1203 (2012) 053. arXiv:1201.2423, doi:10.1007/JHEP03(2012)053.
[4] M. Cacciari, J. Rojo, G. P. Salam, G. Soyez, Jet reconstruction in heavy ion collisions, Eur.Phys.J.C 71 (2010) 1539. arXiv:1010.1759.
[5] G. de Barros, Inclusive Distribution of Fully Reconstructed Jets in Heavy Ion Collisions at RHIC: Status Report, AIP Conf.Proc. 1441 (2012) 825–828. arXiv:1109.4386, doi:10.1063/1.3700690.
[6] G. de Barros, Data-driven analysis methods for the measurement of reconstructed jets in heavy ion collisions at RHIC and LHC, these proceedings.
[7] T. Sjostrand, S. Mrenna, P. Skands, PYTHIA 6.4 physics and manual, JHEP 05 (2006) 026. arXiv:hep-ph/0603175.
[8] K. C. Zapp, F. Krauss, U. A. Wiedemann, Explaining jet quenching with perturbative QCD alone. arXiv:1111.6838.
[9] K. C. Zapp, private communication.